THE JOURNAL OF BIOLOGICAL CHEMISTRY Vol. 279, No. 33, Issue of August 13, pp. 34705–34714, 2004

Printed in U.S.A.

The $\alpha_2\delta$ Auxiliary Subunit Reduces Affinity of ω-Conotoxins for Recombinant N-type ($Ca_v2.2$) Calcium Channels*

Received for publication, October 2, 2003, and in revised form, May 26, 2004
Published, JBC Papers in Press, May 27, 2004, DOI 10.1074/jbc.M310848200

Jorgen Mould‡§¶, Takahiro Yasuda§¶, Christina I. Schroeder‡, Aaron M. Beedle‖, Clinton J. Doering‖‡‡, Gerald W. Zamponi‖§§, David J. Adams§, and Richard J. Lewis‡§¶¶**

From the ‡Institute for Molecular Bioscience and the §School of Biomedical Sciences, The University of Queensland, Queensland 4072, Australia and the ‖Department of Physiology and Biophysics, Cellular and Molecular Neurobiology Research Group, University of Calgary, Calgary, Alberta T2N 4N1, Canada

The ω-conotoxins from fish-hunting cone snails are potent inhibitors of voltage-gated calcium channels. The ω-conotoxins MVIIA and CVID are selective N-type calcium channel inhibitors with potential in the treatment of chronic pain. The β and $\alpha_2\delta$-1 auxiliary subunits influence the expression and characteristics of the α_{1B} subunit of N-type channels and are differentially regulated in disease states, including pain. In this study, we examined the influence of these auxiliary subunits on the ability of the ω-conotoxins GVIA, MVIIA, CVID and analogues to inhibit peripheral and central forms of the rat N-type channels. Although the β3 subunit had little influence on the on- and off-rates of ω-conotoxins, co-expression of $\alpha_2\delta$ with α_{1B} significantly reduced on-rates and equilibrium inhibition at both the central and peripheral isoforms of the N-type channels. The $\alpha_2\delta$ also enhanced the selectivity of MVIIA, but not CVID, for the central isoform. Similar but less pronounced trends were also observed for N-type channels expressed in human embryonic kidney cells. The influence of $\alpha_2\delta$ was not affected by oocyte deglycosylation. The extent of recovery from the ω-conotoxin block was least for GVIA, intermediate for MVIIA, and almost complete for CVID. Application of a hyperpolarizing holding potential (−120 mV) did not significantly enhance the extent of CVID recovery. Interestingly, [R10K]MVIIA and [O10K]GVIA had greater recovery from the block, whereas [K10R]CVID had reduced recovery from the block, indicating that position 10 had an important influence on the extent of ω-conotoxin reversibility. Recovery from CVID block was reduced in the presence of $\alpha_2\delta$ in human embryonic kidney cells and in oocytes expressing $\alpha_{1B\text{-}b}$. These results may have implications for the antinociceptive properties of ω-conotoxins, given that the $\alpha_2\delta$ subunit is up-regulated in certain pain states.

The N-type ($Ca_v2.2$) voltage-gated calcium channels play an important role in the control of neurotransmitter release from nerve terminals (1, 2) and are important drug targets for the treatment of pain (3, 4) and ischemic brain injury (5). Native N-type Ca^{2+} channels are hetero-oligomers that comprise a pore-forming α_1 subunit (α_{1B}) and at least two auxiliary subunits, β and $\alpha_2\delta$, which modulate the α_1 subunit function (6, 7). Two splice variants of the α_{1B} subunit have been identified that occur predominantly in the central ($\alpha_{1B\text{-}d}$) and peripheral ($\alpha_{1B\text{-}b}$) nervous systems (8, 9). Additional splice variants that lack large parts of the domain II-III linker region, including the synaptic protein interaction site, have also been isolated from human brain cDNA libraries (10). Multiple isoforms of the β and $\alpha_2\delta$ subunits also exist that can interact with the α_1 subunit to produce N-type Ca^{2+} channels with different gating properties, allowing the fine tuning of synaptic transmissions (11).

A distinguishing feature of N-type channels is their high sensitivity to block by ω-conotoxins, which are relatively small (~25 residue) polypeptides isolated from the venom of the marine snail of the genus *Conus* (12, 13). ω-Conotoxins have been used as research tools to help define the distribution and physiological roles of specific N-type calcium channels (14–17) and have potential therapeutic value as intrathecal treatments for pain. MVIIA from *Conus magus* is being tested in clinical trials as a treatment for neuropathic pain, but dose-limiting side effects are a concern (18–20). ω-Conotoxin CVID from *Conus catus* (21), which appears to have a wider therapeutic window (22), is also in clinical trials (23).

The modulatory effects of auxiliary subunits on the biophysical properties of Ca^{2+} channel α_1 subunits have been well characterized. When expressed alone, α_1 subunits produce functional channels with kinetic properties that differ substantially from those of the native channel (24, 25). The most commonly observed effect of the β and $\alpha_2\delta$ subunits when they are co-expressed with the α_1 subunit in a heterologous expression system such as *Xenopus* oocytes or HEK[1] 293 cells is to increase the amplitude of macroscopic Ca^{2+} channel currents (typically carried by Ba^{2+} ions) and influence the rate of channel activation and inactivation (26–29). Recently, a negative regulatory effect of the overexpressed β3 subunit on N-type Ca^{2+} channel currents has been demonstrated in *Xenopus* oocytes (30).

* This work was supported by the National Health and Medical Research Council of Australia, an Australian Research Council Special Research Centre for Functional and Applied Genomics Discovery Grant, and operating grants from the Canadian Institutes of Health Research and the Heart and Stroke Foundation of Alberta, the Northwest Territories, and Nunavut (to G. W. Z.). The costs of publication of this article were defrayed in part by the payment of page charges. This article must therefore be hereby marked "*advertisement*" in accordance with 18 U.S.C. Section 1734 solely to indicate this fact.

The atomic coordinates and structure factors (codes 1TTK, 1TT3, 1TTL, and 1TR6) have been deposited in the Protein Data Bank, Research Collaboratory for Structural Bioinformatics, Rutgers University, New Brunswick, NJ (http://www.rcsb.org/).

¶ These authors contributed equally to this work.

** Holder of studentship support from the Alberta Heritage Foundation for Medical Research and the Natural Science and Engineering Research Council of Canada.

‡‡ Supported by an AHFMR studentship.

§§ Canadian Institutes of Health Research Investigator and a Senior Scholar of the Alberta Heritage Foundation for Medical Research.

¶¶ To whom correspondence should be addressed. Tel.: 61-7-33462984; Fax: 61-7-33462101; E-mail: r.lewis@imb.uq.edu.au.

[1] The abbreviations used are: HEK, human embryonic kidney; I-V, current-voltage.

N-type Ca^{2+} channels are widely distributed in brain and peripheral neurons with a variety of co-localized auxiliary subunits (31–34). This heterogeneity in subunit composition contributes to functional and, potentially, to pharmacological heterogeneity. Although the pathophysiological role of auxiliary subunits is poorly understood, up-regulation of $\alpha_2\delta$ subunits has been reported in association with neuropathic pain (35–38). In a previous study, we showed that CVID was a highly selective N-type Ca^{2+} channel inhibitor (21) that inhibited nerve-evoked transmitter release at preganglionic parasympathetic nerve terminals (15). Both CVID and MVIIA inhibited currents mediated by the central and peripheral isoforms of the α_{1B} subunit expressed in *Xenopus* oocytes in the absence of the $\alpha_2\delta$ auxiliary subunit (21). In the present study, we show that the affinity of the ω-conotoxins CVID and MVIIA to block N-type Ca^{2+} channel current is reduced in the presence of $\alpha_2\delta$, and we identify position 10 in ω-conotoxins as having an important influence on the extent of recovery from channel block.

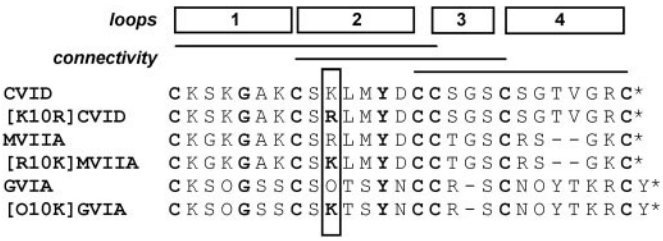

FIG. 1. **Amino acid sequence alignment of the ω-conotoxins CVID (from *C. catus*), MVIIA (*C. magus*), and GVIA (*C. geographus*) and the analogues [K10R]CVID, [R10K]MVIIA, and [O10K]GVIA.** Shown are the positions of the four loops and the disulfide connectivity that characterize ω-conotoxins. Position 10 residues are *boxed*.

EXPERIMENTAL PROCEDURES

Oocyte Injection and Recording—Oocytes (stages V–VI) were surgically removed from mature *Xenopus laevis* frogs anesthetized by immersion in 0.1% 3-aminobenzoic acid ethyl ester (MS-222). The follicular cell layer was removed by incubating oocytes in Ca^{2+}-free solution containing 96 mM NaCl, 2 mM KCl, 1 mM $MgCl_2$, and 5 mM HEPES (pH 7.4) plus 2 mg/ml collagenase (Sigma type 1) for 2 h at room temperature. Oocytes were rinsed several times, sorted, and maintained at 18 °C in an ND96 storage solution that contained 96 mM NaCl, 2 mM KCl, 1 mM $CaCl_2$, 1 mM $MgCl_2$, 5 mM HEPES, and 5 mM pyruvate plus 50 μg/ml gentamycin (pH 7.4).

cRNA was synthesized *in vitro* from linearized template cDNA using an Ambion mMessage mMachine kit. cDNA encoding the rat central $\alpha_{1B\text{-}d}$ and peripheral $\alpha_{1B\text{-}b}$ isoforms of the N-type Ca^{2+} channel, as well as the rat β3 subunit, were kindly provided by Dr. D. Lipscombe (Brown University, Providence, RI). The rabbit $\alpha_2\delta$ ($\alpha_2\delta$-1) subunit was a gift from Drs. N. Klugbauer and F. Hofmann (Technology University of Munich). Oocytes were injected with 2.5–50 ng of each subunit cRNA using a precision injector (Drummond) as indicated under "Results." For co-expression studies, cRNAs encoding for the α_{1B}, β3, and $\alpha_2\delta$ subunits were injected at a 1:1:1–5 concentration ratio, respectively. Injected cells were maintained in ND96 solution at 18 °C for 2–14 days prior to experiments.

Electrophysiological recordings were made in a solution containing 85 mM tetraethylammonium hydroxide, 5 mM KCl, 5 mM HEPES, and 5 mM $BaCl_2$ adjusted to pH 7.4 with methanesulfonic acid. Depolarization-activated Ba^{2+} currents were recorded using a two-electrode voltage clamp with virtual ground circuit (GeneClamp 500B amplifier; Axon Instruments Inc., Union City, CA). Voltage and current electrodes were filled with 3 M KCl and had resistances that ranged from 0.2–1.0 megaohms in the recording solution. Depolarization-activated Ba^{2+} currents were evoked from a holding potential of either −80 mV or −120 mV by test voltages generated using pCLAMP 8.0 software and a Digidata 1200 series interface (Axon Instruments Inc.). Membrane currents were filtered at 1–2 kHz and sampled at 10 kHz. Capacitative and leak currents were subtracted on-line using a −P/4 pulse protocol. Oocytes were continuously perfused with recording solution at a flow rate of 2 ml/min at room temperature (~22 °C). Cells showing <15% change in current amplitude over a 10-min incubation period were used in these studies to avoid problems associated with current rundown. In an attempt to minimize the contamination of recordings by Ca^{2+}-activated chloride currents, oocytes were injected with 46 nl of 50 mM 1,2-bis(*o*-aminophenoxy)ethane-*N*,*N*,*N*′,*N*′-tetraacetate solution at least 15 min prior to recording. All recordings were performed in a small volume (100 μl) Perspex bath. Deglycosylation of intact *Xenopus* oocytes was performed for 2 h at room temperature followed by overnight incubation at 18 °C in oocyte media with the addition of 10 units of peptide:*N*-glycosidase F. ω-Conotoxins were diluted in recording solution and perfused at a flow rate of 2 ml/min. Recordings were made for at least 5 min in the presence of each toxin until the current amplitude stabilized before washout. For each of the ω-conotoxins studied, the rate of onset of toxin block and the rate of the measurable recovery from block during toxin washout were obtained from single exponential fits to the data using Prism software (GraphPad). The K_d for each toxin was then calculated using Equation 1,

$$K_d = K_{off}/K_{on}\ (\text{M}) \qquad \text{(Eq. 1)}$$

where $K_{off} = 1/\tau_{off}\ (s^{-1})$ and $K_{on} = (1/\tau_{on} - K_{off})/[\text{toxin}]\ (M^{-1}\cdot s^{-1})$.

HEK Cell Expression and Electrophysiology—HEK tsA201 cells were maintained at 37 °C (5% CO_2) in Dulbecco's modified Eagle's medium supplemented with fetal bovine serum, penicillin, and streptomycin (Invitrogen). Cells were split to 10% confluence with trypsin-EDTA and transfected 12 h later with cDNAs encoding α_{1B} (25), β1b, or β3 and green fluorescent protein with or without $\alpha_2\delta$ using a standard calcium phosphate protocol. Cells were moved to 28 °C 24 h after transfection and maintained for up to 7 days. Cells were transferred into 20 mM barium external solution containing 20 mM $BaCl_2$, 1 mM $MgCl_2$, 10 mM HEPES, 40 mM tetraethylammonium chloride, 10 mM glucose, and 65 mM CsCl (pH 7.2) and recorded at room temperature (~22 °C). Borosilicate glass pipettes of ~3-megaohm resistance were filled with a cesium methane sulfonate-based internal solution containing 109 mM $CsCH_3SO_4$, 4 mM $MgCl_2$, 9 mM EGTA, and 9 mM HEPES (pH 7.2). Data were acquired and filtered at 1 kHz with an Axopatch 200B amplifier and pCLAMP 8.0 software (Axon Instruments Inc.). Series resistance was compensated to 90%. Membrane currents were evoked every 15 s by 150-ms test pulses from −100 mV to +10 or +20 mV. Cells were perfused directly with control or toxin-containing bath solutions *via* a custom-built perfusion system allowing complete solution changes in <1 s. Data were leak-subtracted and analyzed with Clampfit 8.0 (Axon Instruments Inc.), and graphed in SigmaPlot 2000 (SPSS Inc.).

Peptide Synthesis—The ω-conotoxins CVID, [K10R]CVID, MVIIA, [R10K]MVIIA, GVIA, and [O10K]GVIA (see Fig. 1) were assembled manually using *t*-butoxycarbonyl chemistry *in situ* neutralization solid-phase peptide synthesis (39), deprotected, cleaved, and purified as described previously (40). The purified reduced peptides were oxidized in aqueous 0.33 M NH_4Oac and 0.5 M guanidine-HCl (pH 7.8) for 2–4 days at 4 °C in the presence of reduced and oxidized glutathione (molar ratio 1:100:10). Oxidized peptides were purified by preparative reversed phase high pressure liquid chromatography (40). Mass spectra were measured on a time-of-flight mass spectrometer (PerSeptive Biosystems) equipped with an electrospray atmospheric pressureionization source.

Radioligand Binding Assays—ω-Conotoxin displacement of ^{125}I-GVIA from rat brain membrane was performed as described previously (41). Data are from at least three experiments, each performed in triplicate.

^{1}H NMR Spectroscopy—All NMR spectra were recorded on a Bruker ARX 500 spectrometer equipped with a *z*-gradient unit or on a Bruker DMX 750 spectrometer equipped with a *x*,*y*,*z*-gradient unit. Peptide concentrations were ~2 mM. Hα chemical shifts were obtained from spectra of CVID, [K10R]CVID, MVIIA, [R10K]MVIIA, GVIA, and [O10K]GVIA in 95% H_2O and 5% D_2O (pH ~3.5) at 293 K. Restraints used for the three-dimensional structure calculations of [R10K]MVIIA, GVIA and [O10K]GVIA were from spectra recorded at 275 and 293 K. Three-dimensional solution structures were calculated using the torsion angle dynamics/simulated annealing protocol in XPLOR version 3.851, as described previously (41).

RESULTS

Effects of β3 and $\alpha_2\delta$ Subunits on the Biophysical Properties of N-type Ca^{2+} Channels Expressed in Oocytes—Depolarization-activated Ba^{2+} currents were recorded in *Xenopus* oocytes

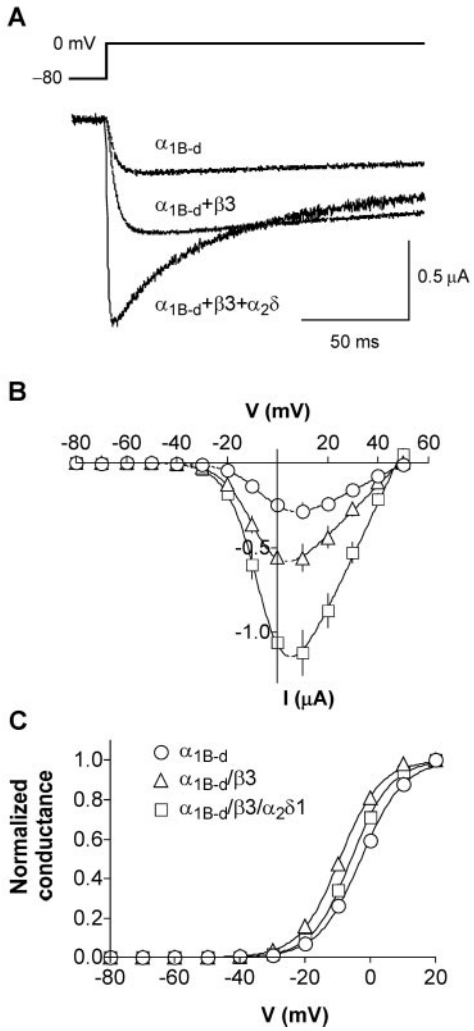

FIG. 2. **The effect of auxiliary subunits on the biophysical properties of the N-type Ca^{2+} channel α_{1B} subunit.** *A*, representative inward Ba^{2+} currents recorded in *Xenopus* oocytes expressing the α_{1B-d} subunit alone or in combination with the β3 and $\alpha_2\delta$ subunits. The *broken line* indicates the zero current level. Currents were evoked by 150-ms voltage steps to 0 mV from a holding potential of −80 mV. Residual capacitive transients after leak subtraction have been erased for clarity. *B*, effect of the β3 and $\alpha_2\delta$ subunits on I-V relationship for α_{1B-d} (n = 11–16 oocytes from 2–3 batches of oocytes). *C*, effect of the β3 and $\alpha_2\delta$ subunits on the voltage dependence of α_{1B-d} activation. Data were derived from the I-V relationships obtained in *B*. Error bars show S.E.

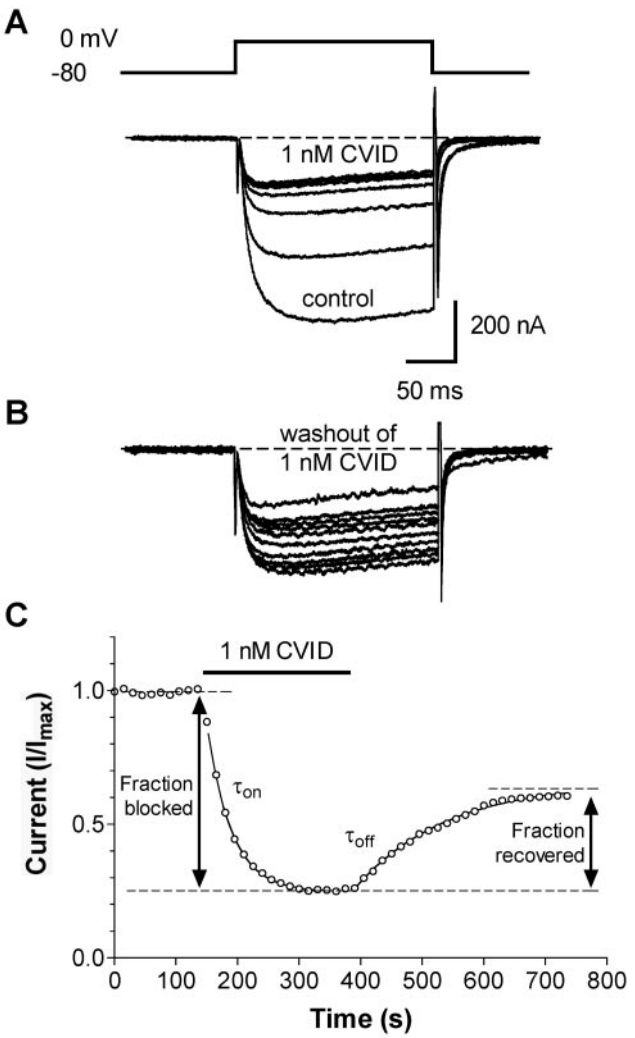

FIG. 3. **Development and recovery from CVID block of N-type channels.** *A*, sequential block of inward Ba^{2+} currents recorded in a *Xenopus* oocyte expressing the peripheral (α_{1B-b}) isoform of the N-type channel in combination with the β3 subunit. Currents were evoked by 200-ms voltage steps to 0 mV from a holding potential of −80 mV. Toxin was added just prior to the first trace (*control*). *B*, currents recorded in the same oocyte during toxin washout. For *A* and *B*, current records were obtained at 15-s intervals but are shown at 30-s intervals for clarity, and *broken lines* indicate the zero current level. *C*, normalized peak current amplitude as a function of time obtained from the traces shown in *A* and *B*. The period of exposure to 1 nM CVID is indicated by the *solid bar*. *Solid lines* are the single exponential fits to the data used to obtain the on- and off-rates. The extent and recovery from block were obtained from these curve fits.

3–5 days following the injection of 2.5 ng of cRNA encoding for the α_{1B-d} (central isoform) of the N-type Ca^{2+} channel (Fig. 2). Currents evoked by 150-ms voltage steps to 0 mV from a holding potential of −80 mV typically ranged from 150–500 nA in peak current amplitude (Fig. 2*A*). Co-expression of the β3 subunit at a 1:1 ratio with α_{1B-d} increased the peak current of current-voltage (I-V) relationships 2-fold compared with α_{1B-d} expressed without the addition of recombinant β3. In agreement with a previous report (8), β3 had only minor effects on the activation and inactivation kinetics of Ca^{2+} channel current (Fig. 2*A*). Co-expression of the β3 subunit caused a significant ($p < 0.001$) hyperpolarizing shift in the half-maximal activation voltage ($V_{½}$) from −2.6 ± 0.8 (n = 11) for α_{1B-d} alone to −8.3 ± 0.8 (n = 16) in the presence of β3 (Fig. 2, *B* and *C*).

Co-expression of the α_{1B-d} and β3 subunits together with the $\alpha_2\delta$ subunit resulted in an additional enhancement of the peak current amplitude (Fig. 2, *A* and *B*). On average, the peak current amplitude from the I-V curve obtained in the presence of the $\alpha_2\delta$ subunit was 2-fold larger than that obtained with the α_{1B-d} + β3 subunit combination alone. Ca^{2+} channel currents recorded from oocytes expressing $\alpha_2\delta$ also exhibited faster activation and inactivation kinetics during the 150-ms test pulse (Fig. 2*A*). Co-expression of $\alpha_2\delta$ + β3 caused a small but significant ($p < 0.01$) depolarizing shift of $V_{½}$ for α_{1B-d} activation to −5.2 ± 0.6 mV (n = 16) compared with β3 alone (−8.3 ± 0.8 mV) (Fig. 2, *B* and *C*). A similar $\alpha_2\delta$-induced depolarizing shift of I-V curves has been reported for N- and R-type Ca^{2+} channels (29, 42). The α_{1B-b} (peripheral isoform) channel current amplitude and channel properties were also modulated by β3 and $\alpha_2\delta$ subunits in a manner similar to their influence on α_{1B-d}.

Effect of β3 and $\alpha_2\delta$ Subunits on the Inhibition by ω-Conotoxins of N-type Ca^{2+} Channel Current Expressed in Oocytes—To assess the influence of different auxiliary subunits on the pharmacology of ω-conotoxins at N-type Ca^{2+} channels, we compared the ability of the ω-conotoxins CVID and MVIIA and

TABLE I

Kinetics and extent of block by the ω-conotoxins CVID, MVIIA, and analogues on the peripheral ($\alpha_{1B\text{-}b}$) N-type Ca^{2+} channel expressed in Xenopus oocytes alone or in combination with β3 and $\alpha_2\delta$ subunits

ω-Conotoxins were applied at 1 nM ($\alpha_{1B\text{-}b}$, $\alpha_{1B\text{-}b}$ + β3) or at 100 nM ($\alpha_{1B\text{-}b}$ + β3 + $\alpha_2\delta$). The extent of recovery from block was determined as described in Fig. 3. Averaged data ± S.E. (n = 5–10 oocytes, as indicated).

Toxin	Amount	Subunits	K_{on}	K_{off}	K_d	Inhibition	Recovery	No.
	nM		$M^{-1}s^{-1} \times 10^7$	$s^{-1} \times 10^{-3}$	nM	%	%	
CVID	1	B-b	0.8 ± 0.1	4.3 ± 0.8	0.58 ± 0.11	40 ± 2	86.9 ± 7.3	5–7
	1	B-b + β3	1.4 ± 0.2	3.7 ± 0.5	0.3 ± 0.06	87.5 ± 3	65.7 ± 8.7	7–8
	100	B-b + β3 + $\alpha_2\delta$	3 ± 0.6 (×10^4)	3.5 ± 0.7	78 ± 17.2	88 ± 5	36.1 ± 5.6	6
[K10R]CVID	1	B-b	2.8 ± 0.5	5.2 ± 0.8	0.18 ± 0.04	69.7 ± 2.6	45 ± 3.9	8
	1	B-b + β3	1.5 ± 0.1	2.9 ± 0.3	0.18 ± 0.02	85 ± 1.9	43.7 ± 5.8	5–9
	100	B-b + β3 + $\alpha_2\delta$	2 ± 0.3 (×10^4)	3 ± 0.7	124 ± 29	91.1 ± 4.6	28.7 ± 3.6	5–6
MVIIA	1	B-b	4.2 ± 0.4	3 ± 1.2	0.2 ± 0.02	65.9 ± 5.7	40.5 ± 5.2	7
	1	B-b + β3	3.5 ± 0.6	4.9 ± 0.4	0.12 ± 0.02	85.3 ± 4	41.9 ± 6.1	10
	100	B-b + β3 + $\alpha_2\delta$	1.8 ± 0.2 (×10^5)	2.1 ± 0.3	18.6 ± 3.8	97.5 ± 0.6	38.3 ± 3.8	5–9
[R10K]MVIIA	1	B-b	4.3 ± 0.6	10.7 ± 1.6	0.24 ± 0.05	69.5 ± 4.3	83.9 ± 7.1	6–8
	1	B-b + β3	4.2 ± 0.5	4.3 ± 0.4	0.11 ± 0.02	72.9 ± 6.5	96.2 ± 4.9	6–8
	100	B-b + β3 + $\alpha_2\delta$	1.2 ± 0.1 (×10^5)	1.8 ± 0.3	15.6 ± 2.6	96 ± 0.3	85.1 ± 16	6

the analogs [K10R]CVID and [R10K]MVIIA (see Fig. 1) to inhibit N-type currents mediated by either α_{1B} alone, α_{1B} + β3, or α_{1B} + β3 + $\alpha_2\delta$. On- and off-rates of channel block and estimates of potency (K_d) for the different Ca^{2+} channel subunit combinations were obtained following application and washout of each toxin (Fig. 3, *A* and *B*). In all cases, the current decrease attributed to toxin block reached a steady state and was fitted by a single exponential function. A single exponential function also fitted recovery from block during toxin washout (Fig. 3*C*). The kinetics, extent, and recovery from block were determined for each toxin from curve fits. Data obtained for the peripheral ($\alpha_{1B\text{-}b}$) and central ($\alpha_{1B\text{-}d}$) isoforms of the N-type Ca^{2+} channel are presented in Tables I and II, respectively.

For the α_{1B} subunit expressed alone or in combination with the β3 subunit, the addition of 1 nM CVID or MVIIA inhibited a substantial portion of the Ba^{2+} current mediated by either the peripheral or the central isoform of the N-type Ca^{2+} channel (Tables I and II). CVID was less potent than MVIIA, especially at the $\alpha_{1B\text{-}d}$ subunit (Tables I and II; Fig. 4*A*). The analogues [K10R]CVID and [R10K] MVIIA had similar profiles of inhibition of α_{1B} to CVID and MVIIA, respectively.

Co-expression of the $\alpha_2\delta$ subunit with α_{1B} + β3 subunit dramatically reduced the apparent affinity of the N-type Ca^{2+} channel for the ω-conotoxins (Figs. 4 and 5), ranging from 150–680-fold at $\alpha_{1B\text{-}b}$ to 80–220-fold at $\alpha_{1B\text{-}d}$ (Tables I and II). At both splice variants, the effect of $\alpha_2\delta$ was most prominent for [K10R]CVID and CVID compared with MVIIA and [R10K]MVIIA. The reduction in potency induced by $\alpha_2\delta$ arose from a markedly reduced on-rate for these ω-conotoxins without any significant effect on off-rate kinetics (Tables I and II; Fig. 5). The same influence of $\alpha_2\delta$ on the kinetics and potency of ω-conotoxin block at α_{1B} were also observed in the absence of the added β3 (Table III). Similar estimates of potency (log IC_{50}) were obtained using equilibrium concentration-response data obtained for ω-conotoxins CVID (−9.93 ± 0.03, −7.66 ± 0.03) and MVIIA (−10.19 ± 0.07, −8.30 ± 0.03) inhibition of $\alpha_{1B\text{-}d}$ + β3 in the absence or presence of $\alpha_2\delta$, respectively (Fig. 4*B*).

Two batches of oocytes expressing $\alpha_{1B\text{-}d}$ + β3 were found to be particularly sensitive to MVIIA block (Fig. 4*B*, *diamonds*); this sensitivity was pronounced when the oocytes were maintained longer and was similar to results obtained previously for CVID at $\alpha_{1B\text{-}d}$ alone (21), indicating that the picomolar inhibition occasionally observed is an oocyte batch-dependent phenomena. Interestingly, a plot of τ_{on} as a function of ω-conotoxin concentration gives a linear relationship with a slope >-1. This difference was most pronounced for τ_{on} obtained in the absence of $\alpha_2\delta$ (−0.48 ± 0.03) but still significantly different from unity in the presence of $\alpha_2\delta$ (−0.73 ± 0.01). Assuming constant off-rate kinetics, this change in the on-rate gives rise to different potency estimates, depending on the concentration of ω-conotoxin tested. In the absence of $\alpha_2\delta$, at 0.1 nM CVID, the estimated K_d was 0.06 nM, whereas at 10 nM CVID the estimated K_d was 20-fold greater (1.3 nM), suggestive of channel heterogeneity.

Reversibility of ω-Conotoxin Inhibition of N-type Ca^{2+} Channel Current Expressed in Oocytes—As observed previously for MVIIA (43, 44), recovery from block (reversibility) for MVIIA and CVID was found to be incomplete (Fig. 6; Tables I and II). For $\alpha_{1B\text{-}b}$ expressed alone, recovery from block was less (~45%) for toxins with Arg at position 10 compared with those with a Lys at position 10 (~ 85%). For $\alpha_{1B\text{-}d}$ channels expressed alone (Table II), CVID and [K10R]CVID had similar levels of recovery (~45%), whereas [R10K]MVIIA (83%) had enhanced recovery compared with MVIIA (25%). For $\alpha_{1B\text{-}b}$ + β3 channels, recovery from block was also greater for peptides containing Arg at position 10, and for $\alpha_{1B\text{-}d}$ + β3 channels it was greater for [R10K]MVIIA. Co-expression of $\alpha_2\delta$ with $\alpha_{1B\text{-}b}$ + β3 further reduced recovery from block for CVID and [K10R]CVID but not for MVIIA and [R10K]MVIIA (Fig. 6, Tables I and II). In contrast, for $\alpha_{1B\text{-}d}$ + β3 + $\alpha_2\delta$ channels the recovery from block was significantly reduced for MVIIA and [R10K]MVIIA but not for CVID and [K10R]CVID. Overall, recovery was least for MVIIA (13%) at $\alpha_{1B\text{-}d}$ and greatest for [R10K]MVIIA at $\alpha_{1B\text{-}b}$ (85%). Previous studies have suggested that the extent of recovery from ω-conotoxin block is enhanced at hyperpolarizing holding potentials (45). In the present study, applying a hyperpolarizing holding potential was found to have no significant influence on the extent of recovery from block, at least for CVID (Table III).

GVIA has a sequence that is distinct from those of other ω-conotoxins (see Fig. 1) and shows pseudo-irreversible binding to the N-type Ca^{2+} channel (45). On the basis that position 10 was found to influence the reversibility of MVIIA and CVID inhibition of N-type calcium channels, we synthesized the analogue [O10K]GVIA to investigate the importance of position 10 for GVIA reversibility. Interestingly, this analogue also showed enhanced reversibility compared with GVIA (Fig. 6, *B* and *C*), suggesting that an interaction between the toxin residue at position 10 and the N-type calcium channel is a key determinant in stabilizing the toxin-bound state.

ω-Conotoxin CVID Inhibition of N-type Ca^{2+} Channel Current Expressed in tsA201 Cells—In contrast to the results ob-

TABLE II

Kinetics and extent of block by the ω-conotoxins CVID, MVIIA, and their analogues on the central ($\alpha_{1B\text{-}d}$) N-type Ca^{2+} channel expressed in Xenopus oocytes alone or in combination with β3 and $\alpha_2\delta$ subunits

ω-Conotoxins were applied at 1 nM ($\alpha_{1B\text{-}d}$, and $\alpha_{1B\text{-}d}$ + β3) or at 100 nM ($\alpha_{1B\text{-}d}$ + β3 + $\alpha_2\delta$). The extent of recovery from block was determined as described in Fig. 3. Averaged data ± S.E. (n = 5–8, as indicated).

Toxin	Amount	Subunits	K_{on}	K_{off}	K_d	Inhibition	Recovery	No.
	nM		$M^{-1}s^{-1} \times 10^7$	$s^{-1} \times 10^{-3}$	nM	%	%	
CVID	1	B-d	1.3 ± 0.3	14.6 ± 2	1.2 ± 0.2	45 ± 5	43 ± 6.4	5
	1	B-d + β3	1.2 ± 0.1	3.7 ± 0.1	0.31 ± 0.04	83.7 ± 7.7	40.5 ± 2.4	8
	100	B-d + β3 + $\alpha_2\delta$	4.5 ± 1.5 (×10^4)	2.71 ± 0.6	48 ± 17	93 ± 3.3	33.6 ± 6.9	7
[K10R]CVID	1	β-d	1.6 ± 0.2	2.7 ± 0.3	0.19 ± 0.05	78.1 ± 6.6	49.2 ± 15	5
	1	β-d + β3	1.5 ± 0.3	2.2 ± .06	0.18 ± 0.04	87.4 ± 2	42.7 ± 10	5
	100	B-d + β3 + $\alpha_2\delta$	4.6 ± 0.27 (×10^4)	1.8 ± .2	39.5 ± 6.3	97.3 ± 3.6	54.4 ± 4.5	6
MVIIA	1	β-d	6 ± 0.8	2.4 ± 0.4	0.04 ± 0.01	73.4 ± 3.9	25.3 ± 2.1	5
	1	B-d + β3	6.3 ± 0.8	4.9 ± 1.1	0.07 ± 0.02	89.7 ± 2.1	46.3 ± 7.6	5–7
	100	B-d + β3 + $\alpha_2\delta$	2.5 ± 0.2 (×10^5)	2.6 ± 1.3	5.7 ± 0.73	96 ± 0.8	13.2 ± 2.6	5
[R10K]MVIIA	1	B-d	4.7 ± 0.6	8.6 ± 1.1	0.16 ± 0.02	88.5 ± 4.5	82.7 ± 5.9	6
	1	B-d + β3	5.8 ± 0.9	5.5 ± 0.8	0.09 ± 0.01	88.7 ± 4.6	87 ± 4.9	6
	100	B-d + β3 + $\alpha_2\delta$	1.6 ± 0.2 (×10^5)	1.4 ± 0.3	8.9 ± 2.2	93.9 ± 0.8	47.8 ± 9.7	5

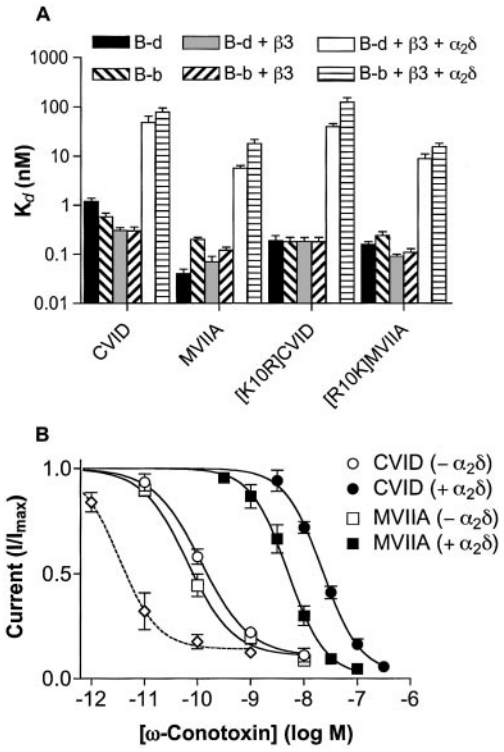

FIG. 4. **Potency of ω-conotoxins at α_{1B} expressed in the presence or absence of β3 and $\alpha_2\delta$.** *A*, potency estimates (K_d) obtained from kinetic data in Tables I and II. *B*, potency estimates obtained from concentration-response curves at $\alpha_{1B\text{-}d}$ (n = 4–8 using six batches of oocytes) produced similar results. Current inhibition for $\alpha_{1B\text{-}d}$ + β3 or $\alpha_{1B\text{-}d}$ + β3 + $\alpha_2\delta$ was evaluated at 7 or 10 min after starting toxin perfusion, respectively (see Fig. 5). Data indicated by the *diamonds* are from two batches of oocytes showing an unusually high sensitivity of $\alpha_{1B\text{-}d}$ + β3 to the block by ω-conotoxin MVIIA (n = 4–7). *Error bars* show S.E.

tained when α_{1B} + β3 was expressed in oocytes where 50% current inhibition was obtained using 0.1–1 nM CV1D, higher concentrations (~100 nM) of CVID were required to inhibit Ba^{2+} currents through α_{1B} + β1b expressed in tsA201 cells (Fig. 7). This reduced potency may be due in part to the differential effects of the β1b and β3 subunits on conotoxin potency or to the higher external Ba^{2+} concentration used as the charge carried in these experiments, which can influence the affinity of ω-conotoxins (for example, compare Refs. 43 and 48). Similar differences in potency between the two expression systems were also observed for MVIIA (data not shown). Consistent with the results obtained in oocytes, coexpression of the $\alpha_2\delta$ subunit reduced CVID affinity, but to a lesser extent (Fig. 7, *A* and *B*). Washout of CVID was again incomplete, especially in the presence of the $\alpha_2\delta$ subunit (Fig. 7*C*).

Radioligand Binding Results—Potencies (pIC_{50}) to displace ^{125}I-GVIA from rat brain membrane were determined to establish whether position 10 changes the affected affinity for native N-type channels found centrally (Table IV). These results showed that the mutated ω-conotoxins had a potency similar to that of their native counterparts at brain N-type calcium channels.

^{1}H NMR and Three-dimensional Structure Calculations—To further probe the role of residue 10 in affinity to oocyte-expressed α_{1B}, ^{1}H NMR was used to identify any structural changes that may be associated with this residue replacement. Comparing Hα chemical shifts with random coil values for a series of related peptides is a sensitive method for identifying changes introduced in the peptide backbone. Replacing residue 10 in MVIIA and GVIA with the corresponding Lys residue from CVID introduced minor changes in the secondary Hα chemical shift in [R10K]MVIIA across residues 10–14, whereas the changes in the secondary Hα chemical shift in [O10K]GVIA were larger in magnitude and spread across residues 8–14. Replacing Lys-10 in CVID with an Arg residue did not result in alterations of the secondary Hα chemical shift (15). Three-dimensional solution structures were calculated for [R10K]MVIIA and [O10K]GVIA, which showed significant secondary Hα chemical shift changes from their native counterparts. Analysis of these structures revealed that replacing Arg-10 in MVIIA with the similar Lys residue did not alter the overall three-dimensional structure of the peptide (Fig. 8*B*), which is consistent with the relatively small changes in the secondary Hα chemical shift observed (Fig. 8*A*). For [O10K]GVIA, which showed larger Hα chemical shift changes, the Hyp to Lys replacement resulted in destabilization of loop 2 residues 9–14 as compared with GVIA. The remainder of the [O10K]GVIA peptide backbone, however, was not perturbed by the Hyp to Lys residue substitution and retained a similar overall structure to GVIA (Fig. 8*B*).

DISCUSSION

The biophysical effects of auxiliary β and $\alpha_2\delta$ subunits on the pore-forming α_1 subunit of calcium channels have been well documented (26, 28, 29, 42). The aim of the present study was to determine how these auxiliary subunits influence the po-

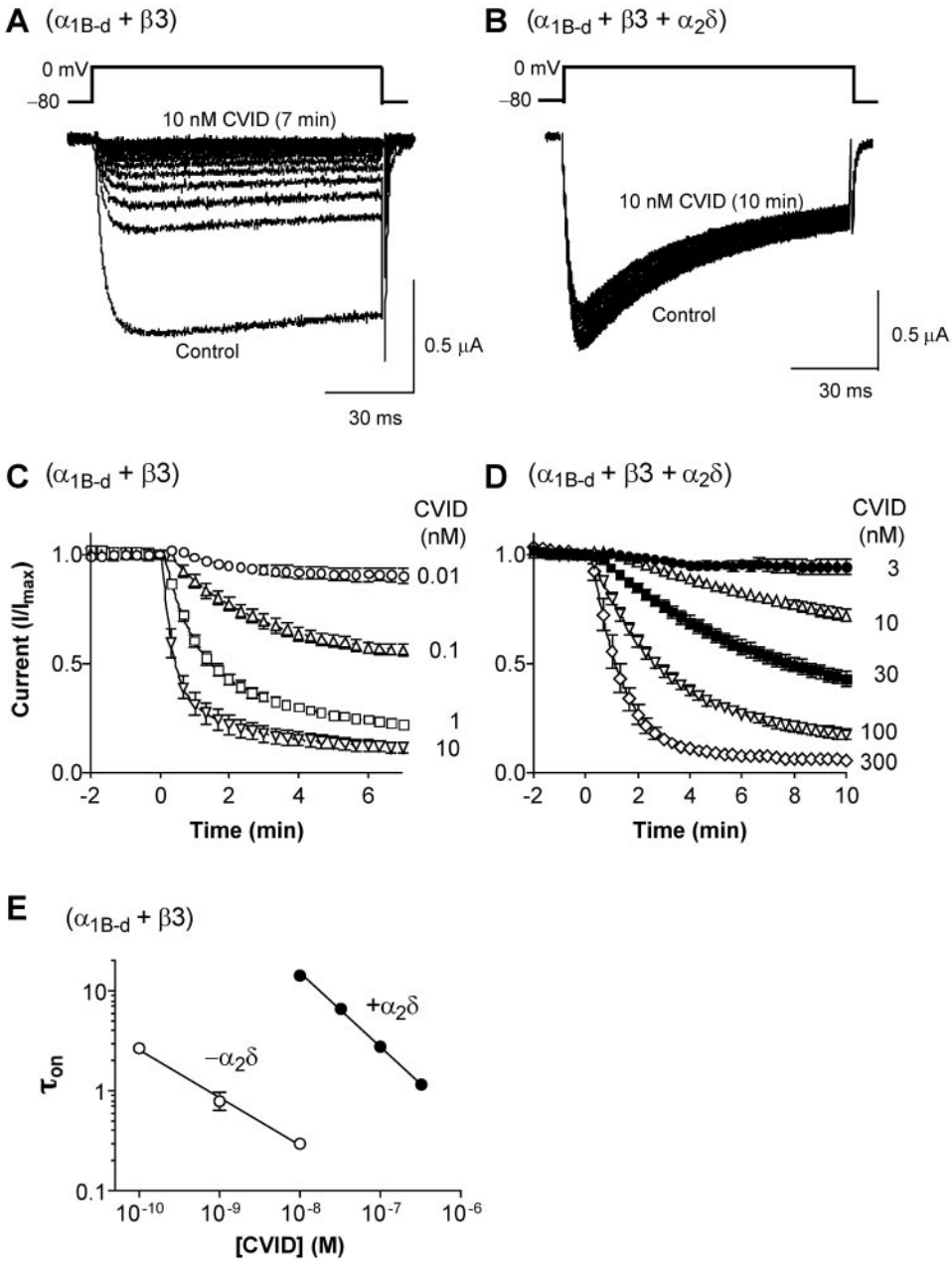

FIG. 5. **Co-expression of $\alpha_2\delta$ decreases the affinity of ω-conotoxins for N-type channels.** *A* and *B*, representative inward Ba^{2+} currents recorded from *Xenopus* oocytes expressing the central isoform (α_{1B-d}) in combination with either the β3 subunit (*A*) or the β3 + $\alpha_2\delta$ subunits (*B*) during a 7- or 10-min application of 10 nM CVID, respectively. Currents were evoked by voltage steps to 0 mV from a holding potential of −80 mV every 20 s. CVID at 10 nM showed robust inhibition of currents through the α_{1B-d} + β3 channel but had little effect on the α_{1B-d} + β3 + $\alpha_2\delta$ combination. *C* and *D*, normalized average peak current amplitude is shown as a function of time obtained from oocytes expressing α_{1B-d} + β3 (*C*) or α_{1B-d} + β3 + $\alpha_2\delta$ (*D*) exposed to different concentrations of CVID. *E*, a plot of the initial on-rate τ_{on} *versus* CVID concentration is fitted by linear relationships. *Error bars* show S.E. (n = 4–8 for each data point using six batches of oocytes).

tency of ω-conotoxins to inhibit currents mediated by N-type ($Ca_v2.2$) calcium channels. Expression of the peripheral (α_{1B-b}) and central (α_{1B-d}) isoforms in *Xenopus* oocytes yielded Ca^{2+} channel currents that were enhanced 2-fold upon co-expression with the β3 subunit. However, the β3 subunit had no significant effect on the ability of the ω-conotoxins CVID, MVIIA, and their analogues to inhibit currents mediated by the α_{1B} subunit. In general, the central α_{1B-d} isoform was more sensitive to block than the peripheral α_{1B-b} isoform for all ω-conotoxins studied, although the maximum difference observed was <5-fold.

In addition to further enhancing the peak current amplitudes of both the central and peripheral isoforms of the N-type Ca^{2+} channel and shifting the $V_{½}$ for activation as observed previously (29), the $\alpha_2\delta$ subunit dramatically reduced ω-conotoxin affinity for N-type channels expressed in oocytes. Co-expression of the $\alpha_2\delta$ subunit together with α_{1B} + β_3 subunits caused a ~100-fold decrease in the sensitivity of the channel to block by CVID, MVIIA, and analogues. K_d values obtained for the inhibition of N-type currents by ω-conotoxin MVIIA in the presence of the $\alpha_2\delta$ subunit were similar to values reported previously (44, 46, 47). The $\alpha_2\delta$ subunit caused a decrease in toxin sensitivity at both the peripheral and central isoforms of the N-type Ca^{2+} channel. In the presence of $\alpha_2\delta$, selectivity for the central over the peripheral isoform was MVIIA ≈ [K10R]CVID > [R10K]MVIIA ≈ CVID (Fig. 4*A*; Tables I and II), indicating that Arg at position 10 contributes to central selectivity. Consistent with the results obtained in *Xenopus*

TABLE III

Kinetics and extent of block by ω-conotoxin CVID at $\alpha_{1B\text{-}d}$ ± β3 at different holding potentials (HP) and after peptide + N-glycosidase F (PNGase F; 10 units) treatment (53)

The extent of recovery from block was determined as described in Fig. 3. Averaged data ± S.E. (n = 4–7 oocytes, as indicated).

[Toxin]	Subunits	HP	K_{on}	K_{off}	K_d	Inhibition	Recovery	No.
nM		*mV*	$M^{-1}s^{-1} \times 10^4$	$s^{-1} \times 10^{-3}$	*nM*	%	%	
1	B-d	−80	1.37 ± 0.09	0.72 ± 0.07	0.052 ± 0.004	62.6 ± 6.9	77 ± 11.4	6
1	B-d	−120	1.33 ± 0.08	0.76 ± 0.14	0.057 ± 0.01	47.9 ± 6	90 ± 6.5	5
100	B-d + $\alpha_2\delta$	−80	3.33 ± 0.29	0.62 ± 0.10	21.1 ± 5.2	89 ± 1.1	19.6 ± 3.9	7
100	B-d + $\alpha_2\delta$	−120	2.71 ± 0.34	0.41 ± 0.47	16.7 ± 3.6	84.4 ± 2.5	31 ± 6.5	5
100	B-d + $\alpha_2\delta$ + PNGase F	−80	3.49 ± 0.16	0.60 ± 0.13	17.5 ± 4.2	87.2 ± 1.3	19.1 ± 3.6	4

oocytes, the $\alpha_2\delta$ subunit also decreased the ω-conotoxin CVID sensitivity of α_{1B} channels expressed in HEK tsA201 cells, although the effect was not as dramatic. This result agrees with an earlier observation in HEK cells in which $\alpha_2\delta$ decreased the affinity to GVIA ~3-fold (48).

Our results demonstrate that the decrease in affinity caused by $\alpha_2\delta$ was achieved through a slowing of the ω-conotoxin association rate (k_{on}). It is possible that this effect may arise from electrostatic shielding or repulsion, perhaps through the proximity of the bulky and heavily glycosylated extracellular α_2 domain to the ω-conotoxin binding site, which presumably resides in the outer vestibule of the channel pore (47). Indeed, oocytes may uniquely glycosylate membrane proteins, thus accounting perhaps for the differences observed between the two expression systems used here. However, the effect of the $\alpha_2\delta$ on ω-conotoxin pharmacology was not influenced by oocyte deglycosylation (Table III). If the effects were indeed due in part to an $\alpha_2\delta$ subunit-induced masking of surface charges, then recording in 20 mM Ba^{2+} would be expected to attenuate any $\alpha_2\delta$ effects due to the increased charge-screening capability of 20 mM Ba^{2+}. Unfortunately, we were unable to directly test this possibility, because currents from α_{1B} expressed in HEK cells in the absence of $\alpha_2\delta$ were too small to measure by using 5 mM Ba^{2+} as the charge carrier. A direct physical restriction of ω-conotoxin's access to its binding site on the N-type Ca^{2+} channel protein seems unlikely, as this would be expected to slow both the association and dissociation rates. In contrast, Felix *et al.* (49) reported that the binding of [^{3}H]PN200–110 to the cardiac L-type (α_{1C}) channel was increased by the α_2 moiety of $\alpha_2\delta$, presumably by affecting the conformation of the α_{1C} subunit. It is therefore possible that the opposite effect occurs at α_{1B}. In addition to decreasing conotoxin sensitivity, coexpression of the $\alpha_2\delta$ subunit reduced the percentage of current recovery from conotoxin block following washout. Surprisingly, this effect appeared to be specific to both the α_{1B} isoform expressed and to the type of toxin used, with the effect being greatest for CVID analogues in cells expressing the peripheral isoform and for MVIIA analogues in cells expressing the central isoform. The reason for this difference in the $\alpha_2\delta$ effect on toxin recovery between α_{1B} isoform is not clear. The effects of $\alpha_2\delta$ on ω-conotoxin affinity appears to be unrelated to gabapentin action, because application of gabapentin (100 μM) failed to produce any immediate inhibition of $\alpha_{1B\text{-}d}$ + $\alpha_2\delta$ + β3 current expressed in oocytes.[2]

It was previously reported that the sensitivity of $\alpha_{1B\text{-}d}$ to CVID block was two orders of magnitude greater when expressed in the absence of the β3 subunit (21). In the present study, however, only occasional batches of oocytes expressing $\alpha_{1B\text{-}d}$ alone had high ω-conotoxin affinity (~20-fold enhanced; see Fig. 4*B*); in this instance, the affinity was for MVIIA. Apparently, low picomolar affinity is not restricted to CVID and presumably arises from heterogeneity in α_{1B} pharmacology in oocytes, perhaps as a result of post-translational processing

[2] T. Yasuda, D. J Adams, and R. J. Lewis, unpublished observations.

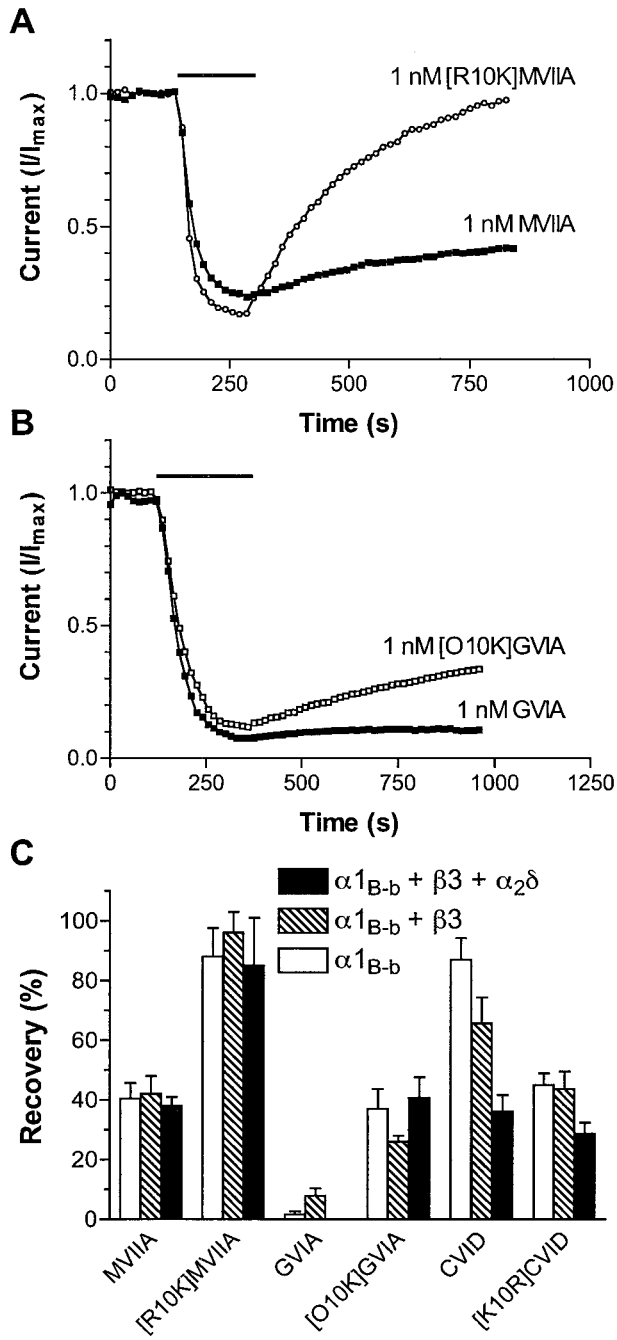

FIG. 6. **Position 10 influences the reversibility of the N-type channel block by ω-conotoxins.** *A* and *B*, normalized peak $\alpha_{1B\text{-}b}$ + β3 current amplitude as a function of time for 1 nM MVIIA and [R10K]MVIIA (*A*) and 1 nM GVIA and [O10K]GVIA (*B*). *C*, the average recovery of current amplitude following washout of ω-conotoxins. Shown are data obtained from oocytes expressing the $\alpha_{1B\text{-}b}$ subunit alone (*solid bars*) or in combination with either the β3 subunit (*hatched bars*) or β3 + $\alpha_2\delta$ subunits (*open bars*). *Error bars* show S.E. ($n \geq 5$).

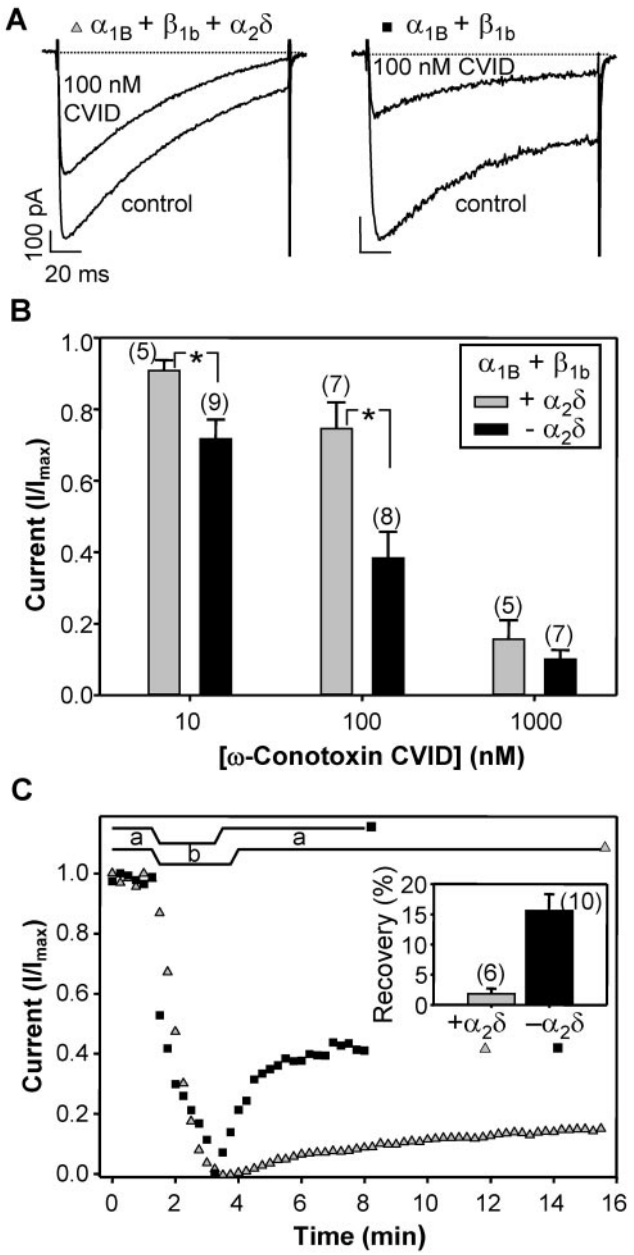

FIG. 7. **ω-Conotoxin block of N-type (α_{1B} + β_{1b}) channel currents transiently expressed in HEK tsA201 cells in the absence or presence of $\alpha_2\delta$.** *A* and *B*, ω-conotoxin CVID inhibition of N-type channels is reduced by the calcium channel $\alpha_2\delta$ subunit. Representative current traces recorded in 20 mM Ba^{2+} external solution depict N-type current block by 100 nM CVID in the presence or absence of $\alpha_2\delta$. *Scale bar labels* correspond to both sets of traces; note different scale bar sizes. Data are plotted as mean ± S.E.; numbers in *parentheses* indicate number of experiments. *Asterisks* indicate $p < 0.05$ in unpaired *t*-tests. *C*, time courses illustrate current reduction by 3 μM CVID (*b*) and recovery during washout (*gray triangles*, $+\alpha_2\delta$; *black squares*, $-\alpha_2\delta$) with 20 mM Ba^{2+} external solution (*a*). *Inset* shows that the percentage of current recovery from CVID block after 2 min of washing is greater in cells lacking the $\alpha_2\delta$ subunit (*black*) than in $\alpha_2\delta$-expressing cells (*gray*).

TABLE IV
Potency to displace ^{125}I-GVIA from rat brain membranes

ω-Conotoxin	Potency (pIC_{50})	95% CI[a]
	M	
CVID	10.42	10.32–10.52
[K10R]CVID	10.24	10.14–10.33
MVIIA	10.71	10.66–10.77
[R10K]MVIIA	10.60	10.50–10.70
GVIA	10.55	10.45–10.63
[O10K]GVIA	10.73	10.64–10.82

[a] Confidence interval.

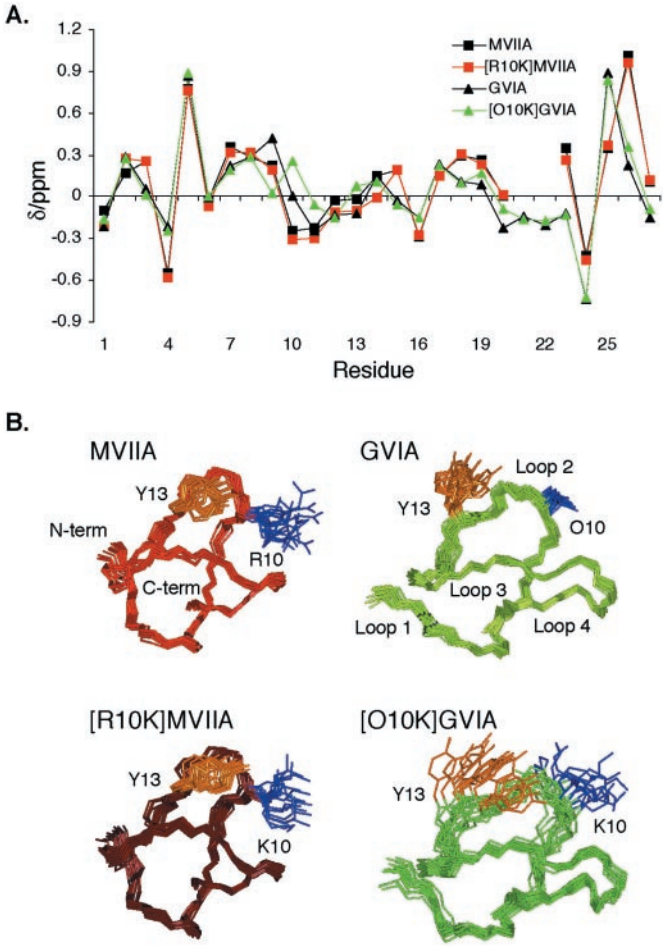

FIG. 8. **^{1}H NMR studies.** *A*, Hα chemical shift for the three residue 10-substituted ω-conotoxins and their native counterparts. *B*, three-dimensional solution structures of MVIIA (accession number RCSB022889; Protein Data Bank (PDB) code 1TTK) (15), [R10K]MVIIA (accession number RCSB02280; PDB code 1TT3) (15), GVIA (accession number RCSB0228890; PDB code 1TTL), and [O10K]GVIA (accession number RCSB022862; PDB code 1TR6). Superimposition of the 20 lowest energy conformations across the entire backbone are shown with the exception of [O10K]GVIA, which was superimposed over residues 1–9 and 15–27.

or auxiliary protein heterogeneity. Similar potency differences were also obtained when K_d estimates at $\alpha_{1B\text{-}d}$ expressed alone were calculated using on-rates of block determined at different concentrations of CVID, which is again suggestive of heterogeneity in α_{1B} pharmacology in oocytes.

In addition to the effect of auxiliary subunits on toxin potency, an overall difference in the extent of recovery from block by different ω-conotoxins was also observed. Recovery from block by CVID was greater than that for MVIIA, whereas GVIA block was virtually irreversible. Interestingly, CVID reversibility was reduced for the peripheral form of the N-type channel in the presence of $\alpha_2\delta$, whereas MVIIA reversibility was reduced at the central form in the presence of $\alpha_2\delta$. In the spinal cord, this difference may allow CVID to preferentially inhibit the ascending presynaptic transmission presumably driven by peripheral subtypes and permit MVIIA to preferentially inhibit the postsynaptic and descending presynaptic transmission presumably driven by central subtypes. A 3-fold preference for the central isoform displayed by MVIIA (but not CVID) is expected to further increase such central selectivity. Central *versus* pe-

ripheral selectivity may have relevance to pain management, given that a dorsal root ganglion-specific splice variant of the N-type calcium channel has recently been identified in peripheral pain pathways (50). It is possible that the selectivity of MVIIA for central isoforms of the N-type calcium channel may explain why it has a narrower therapeutic window than CVID in rat models of inflammatory (22) and neuropathic pain (51).

In an attempt to identify which residues on ω-conotoxins influence reversibility, we investigated a number of position 10 mutants that had previously been identified as influencing calcium channel selectivity (15). [R10K]MVIIA had enhanced reversibility as compared with MVIIA for both the central and peripheral isoforms of the N-type Ca^{2+} channel. Relative to CVID, [K10R]CVID had diminished reversibility at the peripheral isoform of the N-type Ca^{2+} channel or little influence at the central isoform. The influence of position 10 on toxin reversibility was extended to GVIA, with [O10K]GVIA showing enhanced recovery. Taken together, these results suggest that position 10 is a key determinant of ω-conotoxin reversibility. This effect appears to take place through a specific interaction between residue 10 of the toxin and another residue on the N-type Ca^{2+} channel protein, because the shape of the toxin is little altered but apparently more flexible in the mutants. Regions of the a_{1B} subunit crucial for the binding of GVIA in the external vestibule of the channel (domain III; S5-S6 region) have been identified (52). In a recent study by Feng *et al.* (47), residue Gly-1326 was found to be a major determinant of GVIA and MVIIA binding, as mutation of this residue to a proline rendered a block by these ω-conotoxins fully reversible. In contrast to the $\alpha_2\delta$ subunit, which affected the ω-conotoxin on-rate, position 10 residues had a significant impact on the extent of reversibility of ω-conotoxins, irrespective of the auxiliary subunit present.

Replacement of Lys10 in ω-conotoxins CVID with Arg-10 did not alter the secondary Hα chemical shifts compared with the parent peptides. In [R10K]MVIIA, the small change in secondary Hα chemical shifts across residues 9–14 did not influence the overall three-dimensional structure as compared with MVIIA. In comparison, replacing the Hyp-10 in GVIA with a Lys destabilized the loop 2 of GVIA. This suggests that removing the ring-constrained Hyp residue removes an important stabilizing interaction within the peptide. The fact that the results of the washout studies showed that this residue replacement in GVIA increased the reversibility of the peptide suggests that GVIA binds to the N-type calcium channel differently than to CVID and MVIIA. This was supported by radioligand binding studies that show no change in binding affinity for [O10K]GVIA to the N-type channels in rat brain as compared with GVIA. Thus, the shape of loop 2 in GVIA clearly has effects on reversibility but not on the displacement of ^{125}I-GVIA from rat brain membrane. This change in reversibility could be due to a loss of strong interactions between residues in loop 2 and the channel following the destabilization of loop 2 in [O10K]GVIA. However, changes observed in the recovery from block by MVIIA are more likely due to changes in the side chain properties introduced by the Arg to Lys substitution, because CVID and [R10K]MVIIA show greater reversibility as compared with [K10R]CVID and MVIIA. Again, there is no difference among these different peptides in their abilities to displace ^{125}I-GVIA from rat brain membrane. These results support the idea that GVIA interacts with the N-type channels through a different pharmacophore as compared with MVIIA and CVID (13).

In summary, we report that the $\alpha_2\delta$ subunit dramatically decreases the sensitivity of N-type calcium channels to block by ω-conotoxins in oocytes, with qualitatively similar results observed for α_{1B} expressed in HEK cells. Furthermore, the recovery from block by the ω-conotoxins MVIIA and GVIA is partly dependent on the nature of the residue at position 10, providing a means to manipulate dissociation kinetics. Given that the $\alpha_2\delta$ subunit is up-regulated in animal models of neuropathic pain (37), differences in potency and recovery from block may influence how effectively ω-conotoxins reverse different painful conditions *in vivo*.

REFERENCES

1. Nowycky, M. C., Fox, A. P., and Tsien, R. W. (1985) *Nature* **316,** 440–443
2. Fox, A. P., Nowycky, M. C., and Tsien, R. W. (1987) *J. Physiol.* **394,** 149–172
3. Malmberg, A. B., and Yaksh, T. L. (1995) *Pain* **60,** 83–90
4. Saegusa, H., Kurihara, T., Zong, S., Kazuno, A., Matsuda, Y., Nonaka, T., Han, W., Toriyama, H., and Tanabe, T. (2001) *EMBO J.* **20,** 2349–2356
5. Yamada, K., Teraoka, T., Morita, S., Hasegawa, T., and Nabeshima, T. (1994) *Neuropharmacology* **33,** 251–254
6. McEnery, M.W., Snowman, A. M., Sharp A. H., Adams M. E., and Snyder S. H. (1991) *Proc. Natl. Acad. Sci. U. S. A.* **88,** 11095–11099
7. Witcher, D. R., De Waard, M., Sakamoto, J., Franzini-Armstrong, C., Pragnell, M., Kahl, S. D., and Campbell, K. P. (1993) *Science* **261,** 486–489
8. Lin, Z., Haus, S., Edgerton, J., and Lipscombe, D. (1997) *Neuron* **18,** 153–166
9. Lin, Z., Lin, Y., Schorge, S., Pan, J. Q., Beierlein, M., and Lipscombe, D. (1999) *J. Neurosci.* **19,** 5322–5331
10. Kaneko, S., Cooper, C. B., Nishioka, N., Yamasaki, H., Suzuki, A., Jarvis, S. E., Akaike, A., Satoh, M., and Zamponi, G. W. (2002) *J. Neurosci.* **22,** 82–92
11. Wu, L. G., Westenbroek, R. E., Borst, J. G., Catterall, W. A., and Sakmann, B. (1999) *J. Neurosci.* **19,** 726–736
12. Olivera, B. M., Miljanich, G. P., Ramachandran, J., and Adams, M. E. (1994) *Annu. Rev. Biochem.* **63,** 823–867
13. Nielsen, K. J., Schroeder, T., and Lewis, R. (2000) *J. Mol. Recognit.* **13,** 55–70
14. Adams, M. E., Myers, R. A., Imperial, J. S., and Olivera, B. M. (1993) *Biochemistry* **32,** 12566–12570
15. Adams, D. J., Smith, A. B., Schroeder, C. I., Yasuda, T., and Lewis, R. J. (2003) *J. Biol. Chem.* **278,** 4057–4062
16. Tsien, R. W., Ellinor, P. T., and Horne, W. A. (1991) *Trends Pharmacol. Sci.* **12,** 349–354
17. Dunlap, K., Luebke, J. I., and Turner, T. J. (1994) *Science* **266,** 828–831
18. Atanassoff, P. G., Hartmannsgruber, M. W., Thrasher, J., Wermeling, D., Longton, W., Gaeta, R., Singh, T., Mayo, M., McGuire, D., and Luther, R. R. (2000) *Reg. Anesth. Pain Med.* **25,** 274–278
19. Jain, K. K. (2000) *Expert Opin. Investig. Drugs* **9,** 2403–2410
20. Levin, T., Petrides, G., Weiner, J., Saravay, S., Multz, A. S., and Bailine, S. (2002) *Psychosomatics* **43,** 63–66
21. Lewis, R. J., Nielsen, K. J., Craik, D. J., Loughnan, M. L., Adams, D. A., Sharpe, I. A., Luchian, T., Adams, D. J., Bond, T., Thomas, L., Jones, A., Matheson, J. L., Drinkwater, R., Andrews, P. R., and Alewood, P. F. (2000) *J. Biol. Chem.* **275,** 35335–35344
22. Smith M. T., Cabot P. J., Ross F. B., Robertson A. D., and Lewis R. J. (2002) *Pain* **96,** 119–127
23. Cousins M. J., Goucke R. C., Cher, L. M., Brooker, C. D., Amor. P. E., and Crump D. E. (2003) in *Proceedings of the 10th World Congress on Pain: Progress in Pain Research and Management, San Diego, CA, August 17–22, 2002* (Dostrovsky, J. O., Carr, D. B., and Koltzenburg, M. D.) pp. A615–P249, International Association for the Study of Pain, Seattle, WA
24. Lacerda, A. E., Kim, H. S., Ruth, P., Perez-Reyes, E., Flockerzi, V., Hofmann, F., Birnbaumer, L., and Brown, A. M. (1991) *Nature* **352,** 527–530
25. Stea, A., Dubel, S. J., Pragnell, M., Leonard, J. P., Campbell, K. P., and Snutch, T. P. (1993) *Neuropharmacology* **32,** 1103–1116
26. De Waard, M., and Campbell, K. P. (1995) *J. Physiol.* **485,** 619–634
27. Birnbaumer, L., Qin, N., Olcese, R., Tareilus, E., Platano, D., Costantin, J., and Stefani, E. (1998) *J. Bioenerg. Biomembr.* **30,** 357–375
28. Jones, L. P., Wei, S. K., and Yue, D. T. (1998) *J. Gen. Physiol.* **112,** 125–143
29. Wakamori, M., Mikala, G., and Mori, Y. (1999) *J. Physiol.* **517,** 659–672
30. Yasuda, T., Lewis, R. J., and Adams, D. J. (2004) *J. Gen. Physiol.* **123,** 401–416
31. Tanaka, O., Sakagami, H., and Kondo, H. (1995) *Brain Res. Mol. Brain Res.* **30,** 1–16
32. Ludwig, A., Flockerzi, V., and Hofmann, F. (1997) *J. Neurosci.* **17,** 1339–1349
33. Vance, C. L., Begg, C. M., Lee, W. L., Haase, H., Copeland, T. D., and McEnery, M. W. (1998) *J. Biol. Chem.* **273,** 14495–14502
34. Kim, D. S., Yoon, C. H., Lee, S. J., Park, S. Y., Yoo, H. J., and Cho, H. J. (2001) *Brain Res. Mol. Brain Res.* **96,** 151–156
35. Newton, R. A., Bingham, S., Case, P. C., Sanger, G. J., and Lawson, S. N. (2001) *Brain Res. Mol. Brain Res.* **95,** 1–8
36. Abe, M., Kurihara, T., Han, W., Shinomiya, K., and Tanabe, T. (2002) *Spine* **27,** 1517–1524
37. Luo, Z. D., Calcutt, N. A., Higuera, E. S., Valder, C. R., Song, Y. H., Svensson, C. I., and Myers, R. R. (2002) *J. Pharmacol. Exp. Ther.* **303,** 1199–1205
38. Xiao, H. S., Huang, Q. H., Zhang, F. X., Bao, L., Lu, Y. J., Guo, C., Yang, L., Huang, W. J., Fu, G., Xu, S. H., Cheng, X. P., Yan, Q., Zhu, Z. D., Zhang, X., Chen, Z., and Han, Z. G. (2002) *Proc. Natl. Acad. Sci. U. S. A.* **99,** 8360–8365
39. Schnolzer, M., Alewood, P., Jones, A., Alewood, D., and Kent, S. B. (1992) *Int. J. Pept. Protein Res.* **40,** 180–193
40. Nielsen, K. J., Adams, D., Thomas, L., Bond, T., Alewood, P. F., Craik, D. J., and Lewis R. J. (1999) *J. Mol. Biol.* **289,** 1405–1421
41. Nielsen, K. J., Adams, D. A., Alewood, P. F., Lewis R. J., Thomas L., Schroeder, T., and Craik, D. J. (1999) *Biochemistry* **38,** 6741–6751
42. Qin, N., Olcese, R., Stefani, E., and Birnbaumer, L. (1998) *Am. J. Physiol.* **274,**

C1324–C1331
43. Feng, Z. P., Doering, C. J., Winkfein, R. J., Beedle, A. M., Spafford, J. D., and Zamponi, G. W. (2003) *J. Biol. Chem.* **278,** 20171–20178
44. Stocker, J. W., Nadasdi, L., Aldrich, R. W., and Tsien, R. W. (1997) *J. Neurosci.* **17,** 3002–3013
45. Neely, A., Wei, X., Olcese, R., Birnbaumer, L., and Stefani, E. (1993) *Science* **262,** 575–578
46. Meadows, H.,J., and Benham, C.,D. (1999) *Ann. N. Y. Acad. Sci.* **868,** 224–227
47. Feng, Z. P., Hamid, J., Doering, C., Bosey, G. M., Snutch, T. P., and Zamponi, G. W. (2001) *J. Biol. Chem.* **276,** 15728–15735
48. Brust, P. F., Simerson, S., McCue, A. F., Deal, C. R., Schoonmaker, S., Williams, M. E., Velicelebi, G., Johnson, E. C., Harpold, M. M., and Ellis, S. B. (1993) *Neuropharmacology* **32,** 1089–1102
49. Felix, R., Gurnett, C. A., De Waard, M., and Campbell, K. P. (1997) *J. Neurosci.* **17,** 6884–6891
50. Bell, T. J., Thaler, C., Castiglioni, A. J., Helton, T. D., and Lipscombe, D. (2004) *Neuron* **41,** 127–138
51. Scott, D. A., Wright, C. E., and Angus, J. A. (2002) *Eur. J. Pharmacol.* **451,** 279–286
52. Ellinor, P. T., Zhang, J. F., Horne, W. A., and Tsien, R. W. (1994) *Nature* **372,** 272–275
53. Gurnett, C. A., De Waard, M., and Campbell, K. P. (1996) *Neuron* **16,** 431–440

The $\alpha_2\delta$ Auxiliary Subunit Reduces Affinity of ω-Conotoxins for Recombinant N-type ($Ca_V2.2$) Calcium Channels

Jorgen Mould, Takahiro Yasuda, Christina I. Schroeder, Aaron M. Beedle, Clinton J. Doering, Gerald W. Zamponi, David J. Adams and Richard J. Lewis

J. Biol. Chem. 2004, 279:34705-34714.
doi: 10.1074/jbc.M310848200 originally published online May 27, 2004
